

Effects of surface texturing on microalgal cell attachment to solid carriers

Yan Cui¹, Wenqiao Yuan^{1*}, Jian Cao²

(1. Department of Biological and Agricultural Engineering, North Carolina State University, Raleigh, NC 27695-7625, USA;

2. Department of Mechanical Engineering, Northwestern University, Evanston, IL 60208-3109, USA)

Abstract: The objective of this study was to understand the role of surface texturing in microalgal cell attachment to solid surfaces. Two microalgal species, *Scenedesmus dimorphus* and *Nannochloropsis oculata*, were studied on solid carriers made of nylon and polycarbonate. Ridge, pillar and groove at micro-scale were engineered on the solid carriers. Cell response to the textured surfaces was separately described by the Cassie and Wenzel models and the contact point theory. Comparison between measured and model-predicted contact angles indicated that the wetting behavior of the textured solid carriers fell into the Wenzel state, which implied that algal cells could fully penetrate into the designed textures, but the adhesion behavior would be dependent on the size and shape of the cell. Experimental results showed that the attachment was preferred when the feature size was close to the diameter of the cell attempting to settle. Larger or smaller feature dimensions had the potential to reduce cellular attachment. The observation was found to qualitatively comply with the contact point theory.

Keywords: algae attachment, algal biofuel, Cassie model, contact point theory, surface texture, Wenzel model

DOI: 10.3965/j.ijabe.20130604.006

Citation: Cui Y, Yuan W Q, Cao J. Effects of surface texturing on microalgal cell attachment to solid carriers. Int J Agric & Biol Eng, 2013; 6(4): 44–54.

1 Introduction

Microalgae are a promising source of biodiesel^[1] and other renewable energy^[2-4] due to their fast growth rates, high lipid contents and tremendous potential for water conservation^[5-7] and CO₂ biofixation^[6,8-11]. However, a bottleneck issue with algae biofuel manufacturing is the lack of cost-effective cell culture and harvesting methods^[12]. It was proposed to grow algae on solid

carriers to reduce the cost of algae production, harvesting and drying^[13-15]. In such methods, after thick layers of algae is accumulated (attached) on the solid carrier surface, the carrier can be lifted slightly off of water surface (for easy algae-water separation) and then algal biomass can be collected mechanically (e.g., scraping). Downstream drying costs can be reduced because of the reduced free water in algae biomass harvested using this method. In contrast, with suspended algae production methods, it is costly to separate algae from water because algae concentration is usually low (e.g., <1%).

Algal attachment to solid surfaces is a complex process that involves the living cell, the substratum interface and the surrounding liquid. Surface properties, which are usually characterized with respect to surface chemistry, topography/texture or roughness, have direct effects on manipulating algal attachment^[16]. Most studies have been focusing on anti-biofouling for marine vessels, to design new coatings with certain surface textures to remove or minimize algal fouling on submerged surfaces^[17-20]. Surface texture is comprised

Received date: 2013-10-15 **Accepted date:** 2013-11-26

Biographies: Yan Cui, PhD. Research focuses on advanced microalgae culture and harvesting. Email: cuiyanwendy@gmail.com. Jian Cao, PhD. Research focuses on deformation-based processes and laser ablation processes. Tel: 1-847-467-1032; Fax: 1-847-491-3915; Email: jcao@northwestern.edu.

***Corresponding author:** Wenqiao Yuan, PhD, Associate Professor, Biological & Agricultural Engineering Department, North Carolina State University. Address: Box 7625, NCSU, Raleigh, NC27695-7625, USA. Research interests: Advanced biofuels and bioproducts, including microalgae culture and bioprocessing, biodiesel, biomass thermochemical conversion, microbial fuel cell, etc. Tel: +1 9195156742; Fax: +1 9195157760; Email: wyuan2@ncsu.edu.

of purposefully designed surface configurations with defined dimensions such as grooves, ridges, pillars, hills, or pores^[21]. A number of researchers studied the attachment of fouling organisms, such as bacteria, diatoms, algal spores and barnacle cyprid, on micro-textured surfaces^[22-30]. These studies indicated that surface textures can be utilized to control cellular attachment, however, the scale of texture required to affect attachment depended on the size and settlement behavior of the target cells^[22].

Despite the large number of papers published in cell attachment to solid carriers, general trends in cell behavior on solid carriers are difficult to establish due to vast differences in cell type, substrate materials, and texture features. The objective of this study was to understand the effect of micro-surface texturing on microalgal cell attachment to solid surfaces. The attachment of two microalgal species, *Scenedesmus dimorphus* and *Nannochloropsis oculata*, on two textured polymers, polycarbonate and nylon were investigated. Three texture patterns including ridge, groove, and pillar were designed on the surfaces of the two polymers.

2 Materials and methods

2.1 Polymer surface texturing

Two polymers, nylon and polycarbonate, were chosen as the solid carrier materials for the proposed semi-immobilized algae culture because of their light weight, low cost, high transparency, and reasonable resistance to seawater corrosion. Another important reason is that these two materials were found to have suitable surface free energies that support the attachment of both *S. dimorphus* and *N. oculata*^[31]. Three types of textures, ridge (Figure 1a), pillar (Figure 1b), and groove (Figure 1c) were designed on both polymer surfaces. Ridges and pillars were generated by imprinting the polymers on a pre-textured metallic mold, which was textured using the laser micromachining center^[32]. Grooves were produced by a desktop micro-rolling mill developed at Cao's group^[33]. The corresponding depth, width and spacing of patterns A, B and C are listed in Table 1. These nominal dimensions were pre-set values in the machines.

2.2 Substrate characterization

Because the samples were not immediately used after surface texturing, it was important to measure the dimensions of the textures in use. A variable pressure scanning electron microscope (VPSEM, Model S3200, Hitachi High Technologies America, Inc., Schaumburg, IL) was used to characterize the surface morphology of textured polymer surfaces. Prior to imaging, the materials were coated with a thin layer of gold-palladium in a sputter coater. It should be noted that these sputter-coated samples were used for VPSEM analysis only but not for subsequent cell culture experiments. The feature size of each pattern was estimated using Revolution software by manually measuring individual diameters across the image. To reveal the depth of the valleys, the specimens were cross cut in liquid nitrogen and analyzed under the VPSEM. The surface topography of pillar-patterned substrata was further characterized by an atomic force microscopy (AFM, model D3000, Digital Instruments, Inc., Tonawanda, NY) to confirm the height of the feature. The scan area (25 $\mu\text{m} \times 25 \mu\text{m}$) was randomly selected for each sample. Commercially available AFM tip was used in the tapping mode. The scan rate was fixed at 0.25 Hz. At least three replications were performed for each measurement and their average values are reported in Table 1.

A comparison between the nominal and measured feature dimensions is shown in Table 1. The first pattern had ridges of 5 μm wide, 1 μm deep and 2 μm apart for both polymers. The second pattern had 2-3 μm high pillars projected from surfaces. Nylon had a major axis of 30 μm , minor axis of 10 μm and spaced between 10 μm to 15 μm apart. Polycarbonate had features of the same major axis, but 15 μm in minor axis and 7-10 μm spacing. The third pattern was groove of 100 μm width. Depth was 10 μm for nylon and 40 μm for polycarbonate due to different material stiffness. Features were separated by 140 μm wide ridge for both materials. As it can be seen from Table 1, the feature sizes were designed in the order of ridge, pillar, and groove, from relatively small to large. The actual dimensions of ridge and groove were similar to their nominal dimensions. However, actual widths of pillars

were quite different from their nominal values probably due to material deformation after being textured.

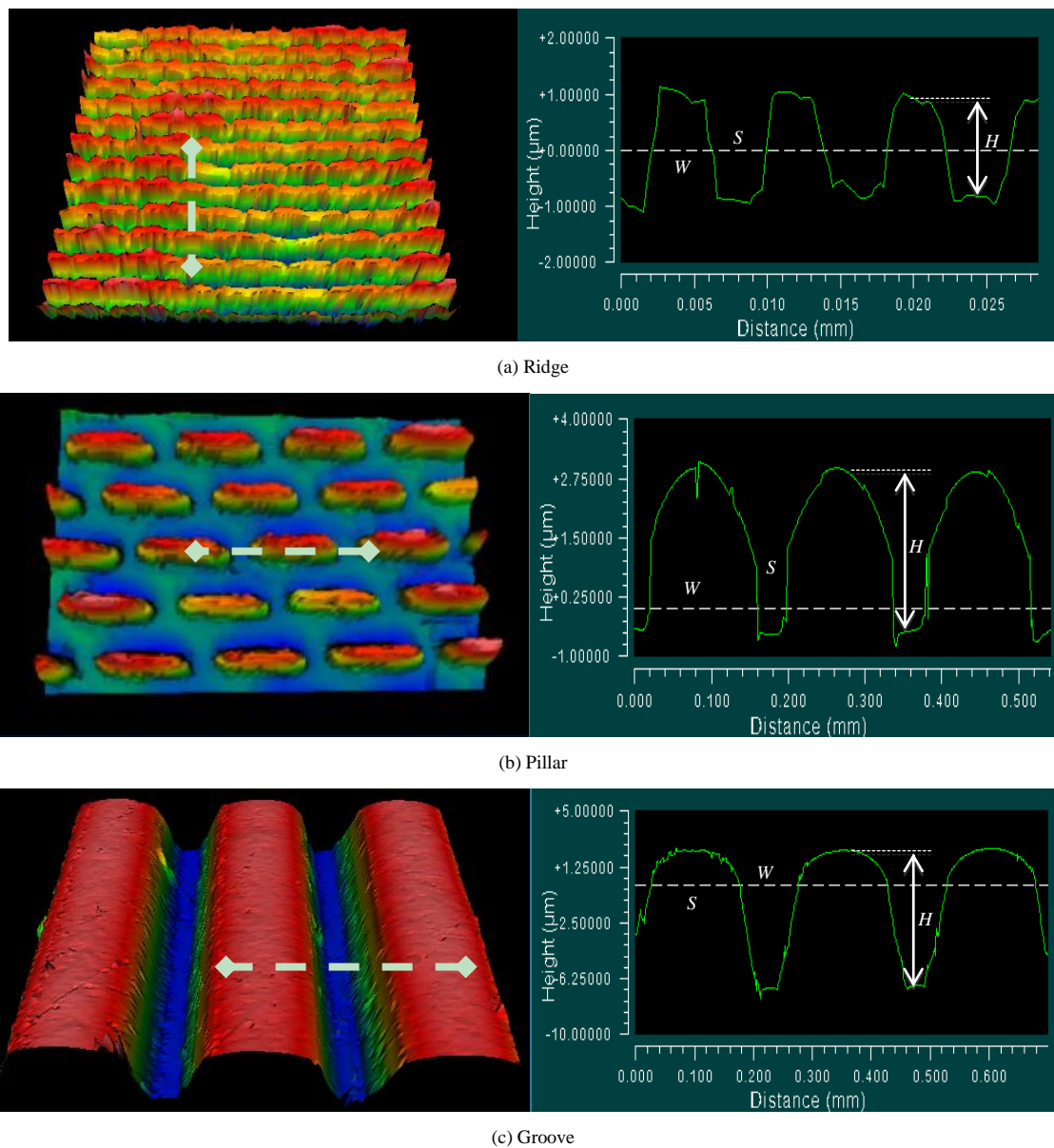


Figure 1 Images of engineered textures on nylon and polycarbonate surfaces: (a) ridge, (b) pillar and (c) groove. H is depth/height, W is width, and S is spacing.

Table 1 Nominal and actual in use dimensions of micro-textured polymers

	Nominal dimensions / μm						Actual dimensions in use / μm					
	Nylon			Polycarbonate			Nylon			Polycarbonate		
	H	W	S	H	W	S	H	W	S	H	W	S
Ridge	2	5	5	2	5	5	1	5	2	1	5	2
Pillar	4	50	14	4	50	14	2-3	30	10-15	2-3	30	7-10
Groove	9	100	140	40	100	140	10	100	140	40	100	140

2.3 Modeling liquid wetting behavior of textured surfaces

Two basic theoretical models were separately developed by Wenzel^[34] and Cassie and Baxter^[35] to explain how surface topography affected liquid wetting

behavior, thus affecting the interface adhesion of cells. In the Wenzel state, a water droplet fully penetrates into the asperities of a textured surface (in wet contact mode), accordingly to pin the droplet, thus generating relatively high adhesion. In contrast, in the Cassie state, the water

droplet is suspended above the asperities (in composite contact mode). Air is trapped between the liquid and the solid substratum. Thus the adhesion of the surface is decreased, and the droplet easily rolls off the surface^[36]. More recently, Quere and colleagues^[37-39] demonstrated an intermediate state between the Wenzel and Cassie states, where a water droplet may partially wet a super-hydrophobic surface. Such an intermediate state is referred to as a metastable state.

A basic parameter in Wenzel's theory is the roughness factor r , which is defined as the ratio of the actual surface of a rough surface to the geometrically projected area as shown in Figure 2. The roughness factor is always larger than 1.0 for a rough surface.

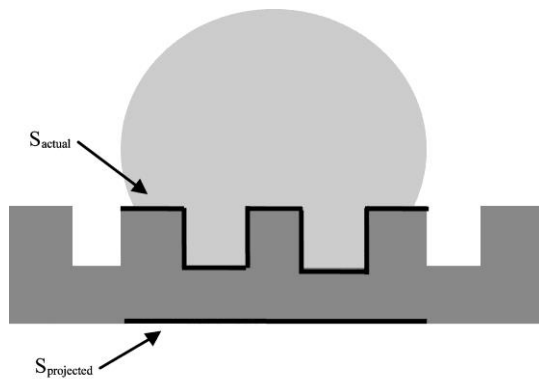


Figure 2 Definition of the Wenzel roughness ratio r related to the wet contact mode.

Wenzel proposed a theoretical equation describing the apparent contact angle on a rough surface as follows^[34]:

$$\cos\theta' = r\cos\theta \quad (1)$$

where, θ' is the apparent contact angle, observed by a given liquid on a rough solid surface. θ refers to the contact angle observed on the corresponding smooth surface.

When the surface is made of small protrusions, which cannot be filled with the liquid and are thus filled with air, the liquid wetting enters the so-called Cassie regime. As a result of the suspension of the water droplet on the asperities, in the Cassie model^[35], the apparent contact angle is described by Equation (2):

$$\cos\theta' = f\cos\theta - 1 - f \quad (2)$$

For a rough surface containing only one type of asperities, given f is the solid fraction (fraction of the surface that is in contact with the liquid), then $(1-f)$ is

the fraction in contact with air (Figure 3).

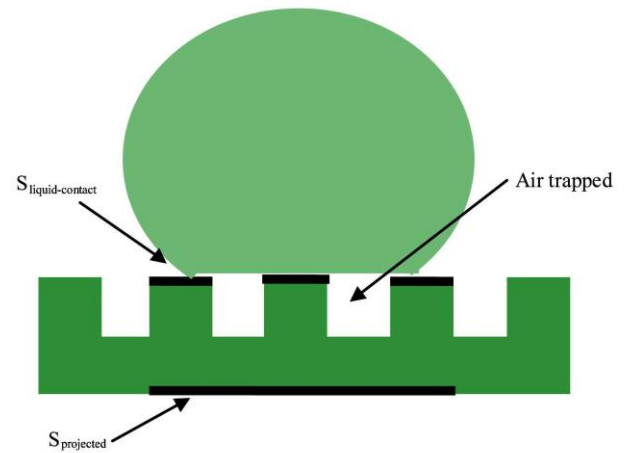


Figure 3 Definition of the Cassie roughness factor f corresponding to the surface fraction of the liquid-solid contact area related to the composite contact mode

2.4 Contact angle measurement

Contact angle was measured on both smooth and textured surfaces using an optical contact angle meter (CAM100, KSV Instrument Ltd., Monroe, CT). Surfaces were cleaned with detergent and ethanol, rinsed exhaustively with distilled water and then air-dried prior to testing with liquid. Micro-liter sized drops of water were placed on the samples, and then the camera coupled with image processing software was used to determine the contact angles. A series of eight drops were used in each of the three trials, for a total of 24 contact angle measurements on a particular material surface.

2.5 Sample preparation and attachment assay

A freshwater microalga *Scenedesmus dimorphus* (UTEX 417) and a marine microalga *Nannochloropsis oculata* (UTEX 2164) were obtained from the University of Texas at Austin Culture Collection of Algae (Austin, TX) and used in the experiments. Both strains are known to contain a large amount of intracellular lipids^[40]. The algae were cultured in 500-mL Erlenmeyer flasks shaken on an orbital shaker at 100 r/min under continuous illumination by cool white fluorescent lamps of 100 to 120 $\mu\text{mol}/(\text{m}^2 \text{ s})$ photons at 12h:12h light:dark periods. The culture temperature was regulated at $(23 \pm 2)^\circ\text{C}$ by in-door air-conditioning. *S. dimorphus* was cultivated in modified Basal medium containing 1.8 g urea, 0.4 g KH_2PO_4 , 0.85 g K_2HPO_4 , 1 g $\text{MgSO}_4 \cdot 7\text{H}_2\text{O}$, 0.5 g EDTA,

0.1142 g H_3BO_3 , 0.111 g $\text{CaCl}_2 \cdot 2\text{H}_2\text{O}$, 49.8 mg $\text{FeSO}_4 \cdot 7\text{H}_2\text{O}$, 88.2 mg $\text{ZnSO}_4 \cdot 7\text{H}_2\text{O}$, 14.2 mg $\text{MnCl}_2 \cdot 4\text{H}_2\text{O}$, 15.7 mg $\text{CuSO}_4 \cdot 5\text{H}_2\text{O}$, and 4.9 mg $\text{Co}(\text{NO}_3)_2 \cdot 6\text{H}_2\text{O}$ in each liter of distilled water. *N. oculata* was grown in modified artificial seawater medium containing the following chemicals in one liter of distilled water: 30 g NaCl, 2.44 g $\text{MgSO}_4 \cdot 7\text{H}_2\text{O}$, 0.6 g KCl, 1 g NaNO_3 , 0.3 g $\text{CaCl}_2 \cdot 2\text{H}_2\text{O}$, 50 mg KH_2PO_4 , 1 g Tricine, 0.27 g NH_4Cl , 1 mL P-IV metal solution, 1 mL vitamin B12, 1 mL Biotin vitamin solution, and 1 mL thiamine vitamin solution. Cells reaching the stationary phase were harvested and diluted with cultured media to approximately 10^5 cells per mL for the attachment experiments.

For the attachment experiments, test panels (3 cm \times 3 cm) were mounted on the microscope glass slides using double-sided tapes. The glass microscope slides with test materials were placed randomly in a glass container and the algae suspension was poured into it. The distance from the top of the suspension to glass slides was 5 cm. The substrata were exposed to the cell suspension for 24 h in the dark without stirring to allow settlement and attachment of cells. Before observation under an optical microscope (BX41, Olympus Inc., Center Valley, PA), the substrata were gently wiped back and forth in distilled water for three times to remove loosely attached and residual suspended cells. Cell attachment was measured as the number of cells attached per unit area. Average counts were made under the microscope for 20 fields of view on each of two replicate slides.

2.6 Statistical analysis

All attachment data were analyzed by SPSS Version 16.0 software (SPSS Inc., USA). Significant differences between all the groups were determined using the Duncan-Waller test. All data presented were mean \pm S.D. and the significance level of 0.05 was applied.

3 Results and discussion

3.1 Contact angle measurement and model comparison

The results obtained by water contact angle measurements were compared to the classic Wenzel and Cassie models to confirm the liquid wetting behavior. The Wenzel model assumes that the liquid wets the

asperities of the rough substrate completely (referred to as wet contact mode), while the Cassie model describes the liquid as sitting on a mixture of air and solid (referred to as composite contact mode).

The contact angles of both smooth and textured surfaces are shown in Table 2, which are also compared with the model-calculated values in Figure 4. All the patterns in this study had relatively low roughness factors ($r = 1.1$ to 1.3) and moderate solid fraction ($f = 0.4$ to 0.7). It can be seen from Figure 4 that the measured contact angles of textured polymers are close to the theoretical curve of Wenzel regime, suggesting that the wetting behavior of these surfaces should follow the full wetting mode proposed by Wenzel rather than by Cassie. The Cassie regime is favored if $\cos\theta + 1r < 0$, which is a simplified criterion for designing super-hydrophobic self-cleaning surfaces^[41,42]. In present study, the calculated values of $(\cos\theta + 1r)$ for all patterns are larger than zero.

Table 2 Measured contact angles on nylon and polycarbonate

Texture	r	f	Contact angle θ ($^\circ$)	Wetting regime	
Nylon	Smooth	1	1	96 \pm 2.3	-
	Ridge	1.286	0.714	105 \pm 8.8	Wenzel
	Pillar	1.23	0.430	91 \pm 4.9	Wenzel
	Groove	1.08	0.583	88 \pm 1.9	Wenzel
Polycarbonate	Smooth	1	1	88 \pm 1.3	-
	Ridge	1.286	0.714	89 \pm 3.7	Wenzel
	Pillar	1.27	0.5	96 \pm 1.4	Wenzel
	Groove	1.33	0.583	84 \pm 3.6	Wenzel

If the topography of a surface is designed to fall into the Cassie regime, air can be trapped between the cell and the rough surface, thus the induced bridging between the cell and solid surface is expected to reduce the overall adhesion strength^[43]. If the topography of a surface is in the Wenzel regime, like in this study, theoretically, cells can fully penetrate into the designed textures but the adhesion behavior is unpredictable in this case. A major reason is that bio-adhesion is a complex process, in which the size and shape of the settled microorganisms are some other factors to consider, in addition to a variety of adhesive proteins, glycoproteins, and polysaccharides that organisms secrete in the adhesion process^[44]. Another theory, the contact point theory^[23] came into place.

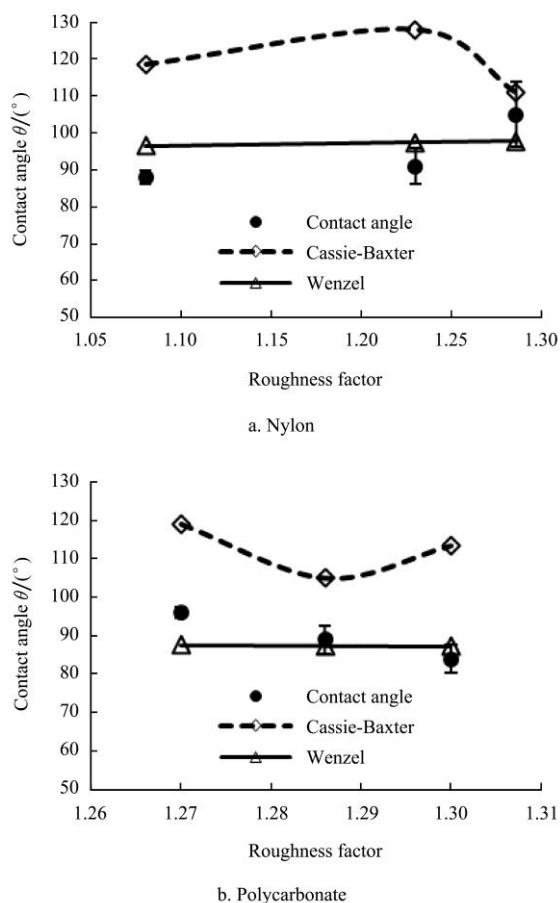


Figure 4 Measured water contact angle of textured polymer as a function of surface roughness factor, compared with the predicted values from Wenzel and Cassie models

3.2 Contact point theory

From the thermodynamic perspective, adhesion on rough surfaces can be simplistically expressed as follows^[23]:

$$W = \gamma \Delta A \quad (3)$$

where, W is the energy needed to realize the adhesion; γ is the solid surface free energy; ΔA is the change of solid surface area. From Equation (3), it can be seen that for a constant surface free energy, the less change of the surface area, the less energy is needed to realize adhesion, thus the easier for a cell to settle. Assuming the chemical composition of a solid material is homogenous (γ is constant), two different surface topographies would be envisioned, i.e., a flat surface and a grooved surface (Figure 5). Considering a cell approaching to the textured surface, it may bridge, align or conform on the surface^[23] (Figure 5). If the cell settles on the flat portion of the surface, there will be an increase in the solid surface area. The increase is the surface area of

the cell minus the contact surface area between the cell and the substratum. Hence, the expansion of the total surface area requires an increase in work exerted on the total system. If the cell is large enough, it may rest between textures depending on the dimensions of the texture (Figure 5). The contacts with the surface become point contact, which would reduce the area of contact between the cell and surface compared to the cell settling on a flat surface. Thus the system would be expected to need more energy for cell attachment. The third condition is that the cell settles into the pattern of the substratum with a particular dimension. It is apparent that the cell has more contact points with the walls and floor of the valley and therefore requires less energy to attach.

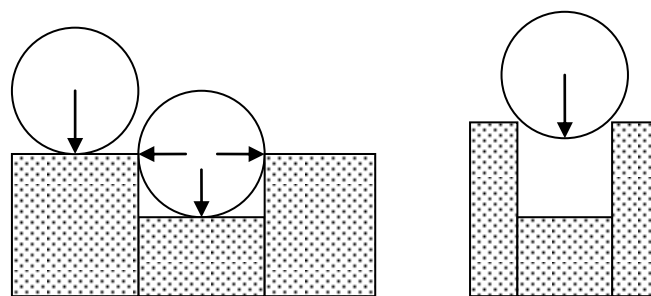


Figure 5 Diagrammatic representation of cell attachment to different surface features. From left to right are aligning, conforming and bridging, respectively^[23].

3.3 Cell attachment to micro-topographies

Experimental results showed that the surface texture had different effects on algal attachment. Independent of surface chemistry, surface texture plays an important role in algal attachment as shown in Figure 6. For smooth surfaces, nylon had a better attachment than polycarbonate for these two algae species due to its relatively low surface free energy as discussed in a previous paper^[31]. The attachment of algal cells to textured surfaces was strongly related to the size of cells and the surface features. Generally, groove had a better attachment than the other two topographies for both algal species. There was no significant difference between pillar and ridge for *N. oculata* attached to both materials, but the attachment of *S. dimorphus* was significantly different. Compared with the smooth control surfaces, *N. oculata* showed reduced attachments on polymers with ridges and pillars, and *S. dimorphus* showed increased

attachment on polycarbonate with pillars while there was reduced attachment on nylon with the same pattern. Polymer with ridges seemed to have no influence on the attachment of *S. dimorphus*.

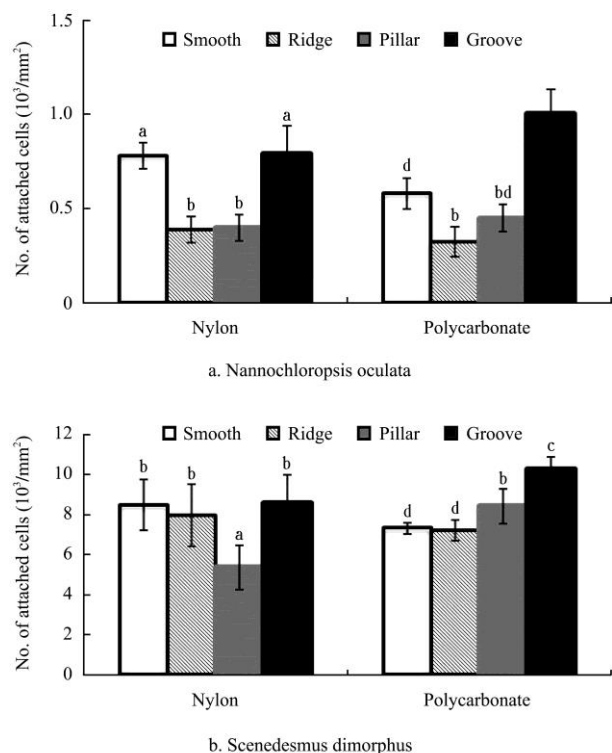


Figure 6 Algal attachment to polymer surfaces with various textures. Different letters above the bars indicate significant differences (Duncan-Waller test, $\alpha = 0.05$)

To understand these differences, the properties of microalgae cells must be taken into consideration. *Scenedesmus dimorphus* is a freshwater unicellular alga with length of 10-16 μm and width of 3-5 μm . Seawater species *Nannochloropsis oculata* is known to be spherically shaped and 2-5 μm in diameter. The ridge spacing was close to the cell size of *Nannochloropsis oculata*, but the depth was only 1 μm so the attachment was still point contact where cells might bridge between or align on the features (Figure 7b and 7d). *S. dimorphus* was larger than the feature size, so bridging became necessary for settlement. According to the contact point theory, cells attach in lower numbers where there are fewer potential contact points. The attachment of *N. oculata* was reduced compared to controlled smooth surfaces due to the decrease of contact points. The shape of *S. dimorphus* allowed for multiple attachment sites, resulting in no big changes in attachment. *S.*

dimorphus was found preferentially oriented with its long axis being perpendicular to the isolated valleys (Figure 7a and 7c). For a bean shaped algal cell like *S. dimorphus*, settling its long axis on the narrow valley reduces contact points between the cell and surface as compared to settling perpendicularly to the valley, which is in qualitative agreement with the contact point theory.

Similar to what were found in this work, previous studies showed that cell behavior had a strong relationship with the valley width^[45]. Very small scratches, smaller than the range of the surface interaction (a few nanometers), had little effect on the local interaction and the overall binding strength. Scratches that are large enough to decrease binding, but too small for the cells to fit into, reduced the contact area of the cells. Valleys that are on the order of the cell size increased the contact area and hence binding potential, while very wide valleys that are much larger than cellular dimensions should approach the binding potential of a flat surface^[45].

For polymer surfaces with pillars, most attached cells were found on flat areas between features against the pillar walls, and there were almost no attached cells on pillars (Figure 8). Feature spacing has been found to be very important in this case. According to the contact point theory, if the spacing is about the size of the algae species, the cell could conform itself into this space. Either larger or smaller feature spacing reduces the contact points thus reduce the adhesion strength. That may explain why polycarbonate with 7-15 μm spacing increased the attachment of *S. dimorphus* while nylon with larger spacing showed reduced attachment. The attachment of *N. oculata* on nylon was significantly reduced due to its smaller size compared to the feature spacing.

The above finding is in agreement with previous studies, which showed that surface micro-topographies smaller than the size of organisms resulted in a reduced adhesion while micro-topographies slightly larger than the size of organisms induced high attachment^[23-25]. Carl et al.^[46] studied the settlement of mussel larvae (approximate width of 190 μm and length of 260 μm) on textured surfaces with feature size ranging from 100 μm

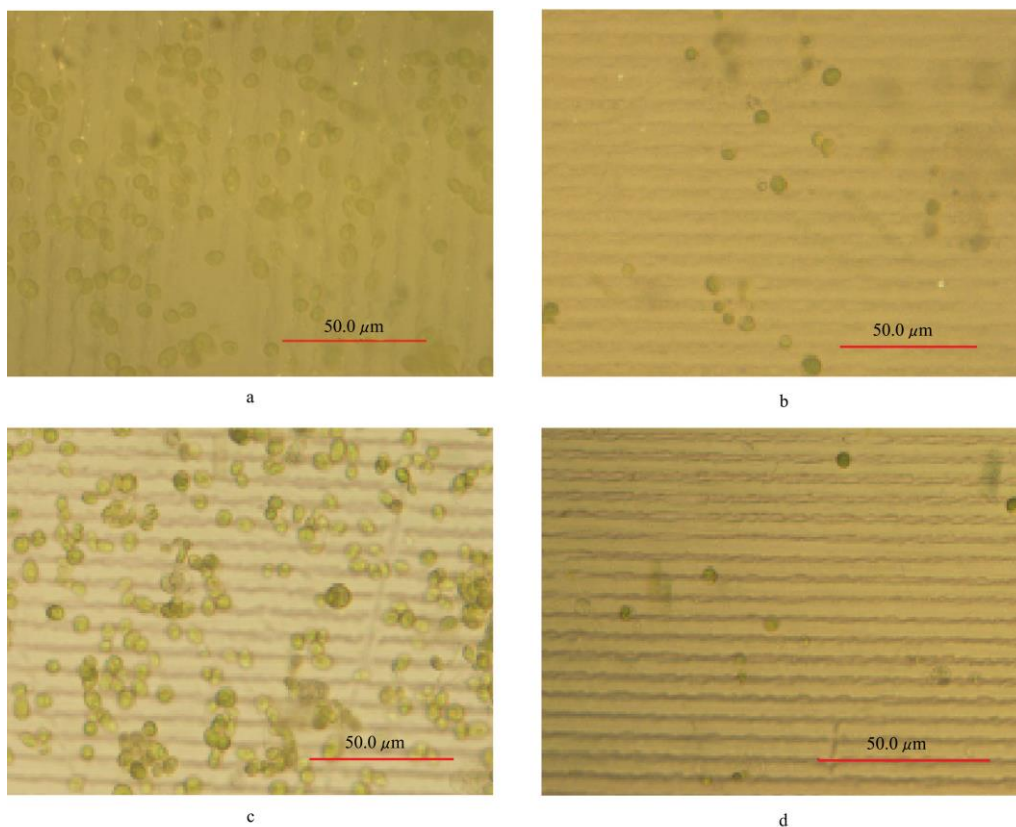


Figure 7 Properties of *S. dimorphus* and *N. oculata* cells

(a) *S. dimorphus* attached on nylon with ridge, (b) *N. oculata* attached on nylon with ridge, (c) *S. dimorphus* attached on polycarbonate with ridge, and (d) *N. oculata* attached on polycarbonate with ridge

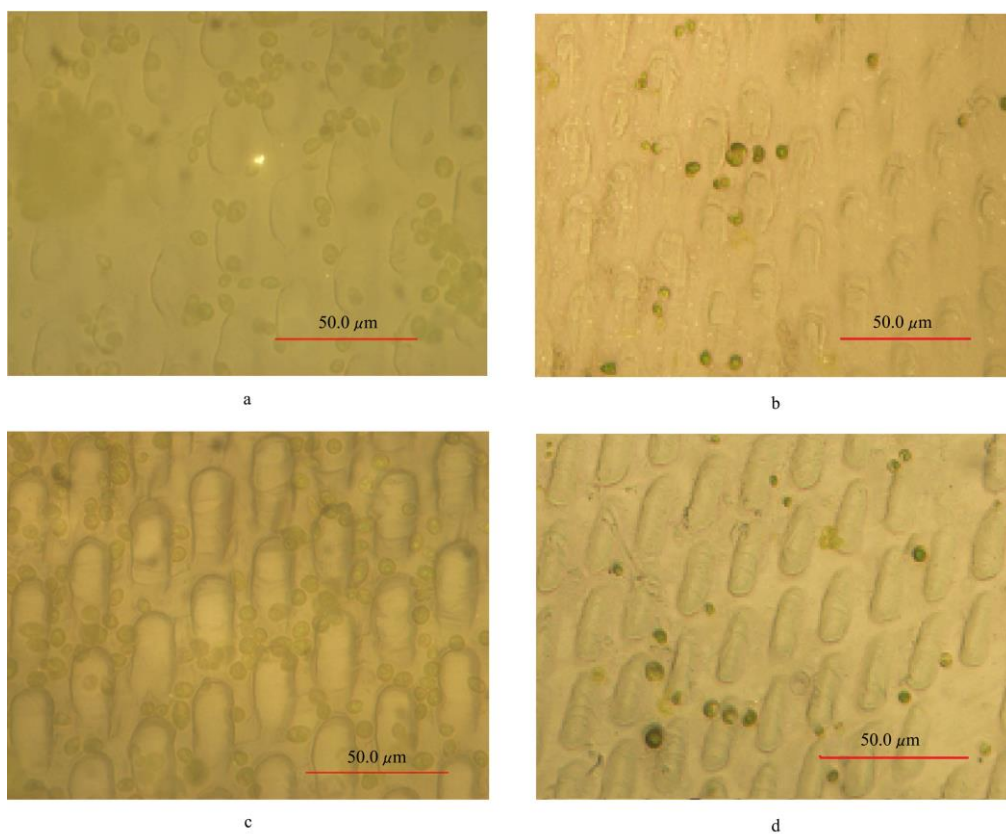


Figure 8 *S. dimorphus* and *N. oculata* cells attached polymer surfaces with pillars

(a) *S. dimorphus* attached on nylon with pillar, (b) *N. oculata* attached on nylon with pillar, (c) *S. dimorphus* attached on polycarbonate with pillar, (d) *N. oculata* attached on polycarbonate with pillar

to 1 000 μm . Decreased settlement was observed on topographies ranging from 100 μm to 250 μm , within this size range larvae was restricted to fit in the features thus impeding the contact area required for optimal adhesion. A similar negative effects of surface topographies, smaller than target organisms, were observed on barnacle *B. improvises* and *B. Amphitrite*^[27,28,47], the serpulid tube worm *Hydroideselegans*^[25], and the bryozoan *Bugulaneritina*^[25]. In contrast, micro-topographies lightly larger than target organisms improved attachment. In the study of mussel larvae attachment, the 400 μm textured surface had the highest settlement, providing more contact points and a more secure settlement site for pediveligers^[46].

The feature dimensions of grooves were much larger than the size of algal cells. Polycarbonate with 40 μm deep grooves increased attachment for both algae species relative to the smooth surface, while nylon with shallower depth showed no big changes in adhesion. Under the microscope, cells were mainly found in the intersection corners between the groove floor and sidewalls. So for two grooves with the same width larger than the cell size, the deeper groove could achieve more cell colonization due to the increased surface area available for cell-substratum contact. Other researchers also reported the similar results. Callow found there was a five-fold increase in algal spore settlement on 5 μm deep valleys as opposed to valleys of 1.5 μm deep^[23]. In the study of mussel larvae, increased settlement was obtained with increasing depth from 200 μm to 400 μm when the groove width was kept around 200 μm ^[46].

4 Conclusions

This study demonstrated that surface texture played an important role in algal attachment by changing the wetting behavior and area of contact between the cell and solid carrier surface. Surface texture in this study was a key factor in the attachment of algal cells to solid carriers, with a greater effect than surface chemistry when the wetting behavior of the surface fell into the Wenzel state (wet contact mode). The contact point theory was applied to examine the interaction between cells and surfaces. Experimental results showed that the

attachment was preferred when the feature size was close to the diameter of the cell attempting to settle, while larger or smaller feature dimensions had the potential to reduce cellular attachment, which were qualitatively consistent with the contact point theory.

Acknowledgements

We would like to thank Dr. Vikas Berry at the Chemical Engineering Department of Kansas State University for the use of the microscope, and Mr. Chuck Mooney at the Analytical Instrument Facility of North Carolina State University for AFM and SEM measurements. This research was financially supported by the U.S. National Science Foundation (Award # CMMI-1239078) and the startup fund of North Carolina State University.

[References]

- [1] Chisti Y. Biodiesel from microalgae. *Biotechnol Advances*, 2007; 25(3): 294-306.
- [2] Donohue T J, Cogdell R J. Microorganisms and clean energy. *Nature Reviews. Microbiology*, 2006; 4(11): 800.
- [3] Schenk P M, Thomas-Hall S R, Stephens E, Marx U C, Mussgnug J H, Posten C, et al. Second generation biofuels: high-efficiency microalgae for biodiesel production. *Bioenergy Research*, 2008; 1(1): 20-43.
- [4] Rodolfi L, Zittelli G C, Bassi N, Padovani G, Biondi N, Bonini G, et al. Microalgae for oil: strain selection, induction of lipid synthesis and outdoor mass cultivation in a low-cost photobioreactor. *Biotechnology Bioengineering*, 2009; 102(1): 100-112.
- [5] Hoffmann J P. Wastewater treatment with suspended and nonsuspended algae. *Journal of Phycology*, 2002; 34(5): 757-763.
- [6] Mata T M, Martins A A, Caetano N S. Microalgae for biodiesel production and other applications: A review. *Renewable and Sustainable Energy Reviews*, 2010; 14(1): 217-232.
- [7] Mehta S K, Gaur J P. Use of algae for removing heavy metal ions from wastewater: progress and prospects. *Critical Reviews in Biotechnology*, 2005; 25(3): 113-152.
- [8] Benemann J R. Bio-fixation of CO₂ and greenhouse gas abatement with microalgae-technology roadmap. Final Report to the US Department of Energy. National Energy Technology Laboratory, 2003.
- [9] Brennan L, Owende P. Biofuels from microalgae-a review of technologies for production, processing, and extractions of

- biofuels and co-products. *Renewable and Sustainable Energy Reviews*, 2010; 14(2): 557-577.
- [10] Lardon L, Helia A, Sialve B, Steyer J P, Bernard O. Life-cycle assessment of biodiesel production from microalgae. *Environmental Science Technology*, 2009; 43(17): 6475-6481.
- [11] Sydney E B, Sturm W, de Carvalho J C, Thomaz-Soccol V, Larroche C, Pandey A, et al. Potential carbon dioxide fixation by industrially important microalgae. *Bioresource Technology*, 2010; 101(15): 5892-5896.
- [12] Molina Grima E, Belarbi E H, Acien Fernandez F G, Robles Medina A, Chisti Y. Recovery of microalgal biomass and metabolites: process options and economics. *Biotechnology Advances*, 2003; 20(7): 491-515.
- [13] Cao J, Yuan W, Pei Z J, Davis T, Cui Y, Beltran M. A preliminary study of the effect of surface texture on algae cell attachment for a mechanical-biological energy manufacturing system. *Journal of Manufacturing Science Engineering*, 2009; 131(6): 064505.1-064505.4.
- [14] Yuan W, Cui Y, Pei Z J. Immobilized algae culture for biofuel manufacturing: an overview and progress report. *Proceedings of 2009 NSF Engineering Research and Innovation Conference, Honolulu, Hawaii, 2009.*
- [15] Cui Y, Yuan W, Pei Z J. Effects of carrier material and design on microalgae attachment for biofuel manufacturing: a literature review. *Proceedings of the ASME 2010 International Manufacturing Science and Engineering Conference, 2010; 1: 525-540.*
- [16] Schumacher J F, Carman M L, Estes T G, Feinberg A W, Wilson L H, Callow M E, et al. Engineered antifouling microtopographies - effect of feature size, geometry, and roughness on settlement of zoospores of the green alga *Ulva*. *Biofouling*, 2007; 23(1): 55-62.
- [17] Magin C M, Cooper S P, Brennan A B. Non-toxic antifouling strategies. *Materials Today*, 2010; 13(4): 36-44.
- [18] Baier R E. Surface behavior of biomaterials: the theta surface for biocompatibility. *Journal of Materials Science: Materials in Medicine*, 2006; 17(11): 1057-1062.
- [19] Baier R E, Meyer A E. Surface analysis of fouling-resistant marine coatings. *Biofouling*, 1992; 6(2): 165-180.
- [20] Anderson C, Atlar M, Callow M, Candries M, Milne A, Townsin R L. The development of foul-release coatings for seagoing vessels. *Journal of Marine Design and Operations*, 2003; 4: 11-23.
- [21] Von Recum A F, Van Kooten T G. The influence of microtopography on cellular response and the implications for silicone implants. *Journal of Biomaterials Science, Polymer Edition*, 1995; 7(2): 181-198.
- [22] Callow M E, Jennings A R, Brennan A B, Seegert C E, Gibson A, Wilson L, et al. Microtopographic cues for settlement of zoospores of the greenfouling alga *Enteromorpha*. *Biofouling*, 2002; 18(3): 237-245.
- [23] Scardino A J, Harvey E, De Nys R. Testing attachment point theory: diatom attachment on microtextured polyimide biomimics. *Biofouling*, 2006; 22(1): 55-60.
- [24] Scardino A J, Guenther J, De Nys R. Attachment point theory revisited: the fouling response to a microtextured matrix. *Biofouling*, 2008; 24(1): 45-53.
- [25] Hoipkemeier-Wilson L, Schumacher J F, Carman M L, Gibson A L, Feinberg A W, Callow M E, et al. Antifouling potential of lubricious, micro-engineered, PDMS elastomers against zoospores of the green alga *Ulva* (*Enteromorpha*). *Biofouling*, 2004; 20(1): 53-63.
- [26] Schumacher J F, Aldred N, Callow M E, Finlay J A, Callow J A, Clare A S, et al. Species-specific engineered antifouling topographies: correlations between the settlement of algal zoospores and barnacle cyprids. *Biofouling*, 2007; 23(5): 307-317.
- [27] Berntsson K M, Jonsson P R, Lejhall M, Gatenholm P. Analysis of behavioural rejection of micro-textured surfaces and implications for recruitment by the barnacle *Balanus improvisus*. *Journal of Experimental Marine Biology and Ecology*, 2000; 251(1): 59-83.
- [28] Kohler J, Hansen P D, Wahl M. Colonization patterns at the substratum-water interface: how does surface microtopography influence recruitment patterns of sessile organisms. *Biofouling*, 1999; 14(3): 237-248.
- [29] Petronis S, Berntsson K, Gold J, Gatenholm P. Design and microstructuring of PDMS surfaces for improved marine biofouling resistance. *Journal of Biomaterials Science, Polymer Edition*, 2000; 11(10): 1051-1072.
- [30] Berntsson K M, Andreasson H, Jonsson P R, Larsson L. Reduction of barnacle recruitment on micro-textured surfaces: analysis of effective topographic characteristics and evaluation of skin friction. *Biofouling*, 2000, 16(2-4): 245-261.
- [31] Cui Y, Yuan W. Thermodynamic modeling of algal cell-solid substrate interactions. *Applied energy*, 2013; 112: 485-492.
- [32] Davis T, Cao J. Effect of laser pulse overlap on machined depth. *Transaction of the North American Manufacturing Research Institution of SME*, 2010; 38: 291-298.
- [33] Zhou R, Cao J, Ehmann K, Xu C. An investigation on deformation-based micro surface texturing. *Journal of Manufacturing Science and Engineering*, 2011; 133(6): 061017.1-061017.6.
- [34] Wenzel R N. Resistance of solid surfaces to wetting by water. *Industrial and Engineering Chemistry*, 1936; 28(8): 988-994.
- [35] Cassie A B D, Baxter S. Wettability of porous surfaces.

- Transaction of the Faraday Society, 1944; 40: 546-551.
- [36] Liu M J, Zheng Y M, Zhai J, Jiang L. Bioinspired super-antiwetting interfaces with special liquid-solid Adhesion. *Accounts of chemical research*, 2009; 43(3): 368-377.
- [37] Bico J, Tordeux C, Quere D. Rough wetting. *Europhysics Letters*, 2007; 55(2): 214-220.
- [38] Bico J, Thiele U, Quere D. Wetting of textured surfaces. *Colloids Surfaces A: Physicochemical and Engineering Aspects*, 2002; 206(1-3): 41-46.
- [39] Quere D. Rough ideas on wetting. *Physica A: Statistical Mechanics and its Applications*, 2002; 313(1-2): 32-46.
- [40] Ben-Amotz A, Tornabene T G, Thomas W H. Chemical profile of selected species of microalgae with emphasis on lipids. *Journal of Phycology*, 1985; 21(1): 72-81.
- [41] Furstner R, Barthlott W. Wetting and self-cleaning properties of artificial superhydrophobic surfaces. *Langmuir*, 2005; 21: 956-961.
- [42] Lafuma A, Quere D. Superhydrophobic states. *Nat Mater*, 2003, 2(7): 457-460.
- [43] Sun T, Feng L, Gao X, Jiang L. Bioinspired Surfaces with Special Wettability. *Accounts of Chemical Research*, 2005; 38(8): 644-652.
- [44] Vladkova T. Surface Modification Approach to Control Biofouling. *Marine and industrial biofouling*, 2009; 4: 135-163.
- [45] Edwards K J, Rutenbergr A D. Microbial response to surface microtopography: the role of metabolism in localized mineral dissolution. *Chemical Geology*, 2001; 180(1): 19-32.
- [46] Carl C, Poole A J, Sexton B A, Glenn F L, Vucko M J, Williams M R, et al. Enhancing the settlement and attachment strength of pediveligers of *Mytilus galloprovincialis* by changing surface wettability and microtopography. *Biofouling*, 2012; 28(2): 175-186.
- [47] Andersson M, Berntsson K, Jonsson P, Gatenholm P. Microtextured surfaces: towards macrofouling resistant coatings. *Biofouling*, 1999; 14: 167-168.